Finite Element Thermal Analysis of Three Dimensionally Printed (3DP™) Metal Matrix Composites

S. Johnston[1,2] and R. Anderson[2*]

[1] Dept. of Mechanical Engineering, University of Washington, Seattle, WA 98195
[2] Concurrent Technologies Corporation, Bremerton, WA 98312
[*] Author to whom correspondence should be addressed.

ABSTRACT

Three Dimensional Printing, 3DP™, is under development for the production of metal composites through solid freeform fabrication of a skeleton, followed by sintering and then infiltration of a second, lower melting metal. To maintain dimensionality and allow for infiltration, green component sintering produces only neck growth between powder particles, which differs substantially from conventional powder metallurgy sintering practices. The objective of this study is to investigate finite element thermal-mechanical modeling in order to optimize the sinter profile and predict the final part dimension. The model will relate micro-scale thermal effects to the macro-scale by analyzing the composite medium as a meshed layered element comprising micro-scale elements. The micro-scale elements can be based on bulk transport mechanisms related to neck growth. The analytical model will eventually be used to define the thermal processing parameters and to predict optimal geometry for full density near net shape sintering and infiltration of 3DP™ manufactured components.

INTRODUCTION

Three Dimensional Printing, 3DP™,[1] is a rapid prototyping and manufacturing process that creates complex three-dimensional parts directly from a computer-aided design (CAD) model. Developed at the Massachusetts Institute of Technology, Three Dimensional Printing is one of several solid freeform technologies for the production of prototypes, functional parts, and tooling. Some of the benefits of the unique technology of 3DP™ include the economic fabrication of small quantity parts and one-offs, the use of alternative materials, and the redesign of parts and assemblies to enhance performance and durability.

The 3DP™ powder metallurgical process involves spreading a thin layer of metal powder over the surface of a part-build bed. Using ink-jet printing technology, a liquid binder material is deposited to selectively join the powder particles where the part is to be formed. The powder bed and part are lowered and a new layer of powder is spread and selectively joined. This layer-by-layer printing process repeats until the part is completed. After thermal processing for debinding and sintering, the fabricated preform, or "skeleton," undergoes infiltration to form a metal matrix composite component that is capable of serving not only as a *prototype* but, depending on the material system and application requirements, as a *fully functional part*.

Understanding the thermal processing mechanisms during sintering is essential to dimensional and surface quality control of 3DP™ components. In contrast to machined, cast, or forged components, 3DP™ powder metallurgical parts require three specific heat treatments before the component is ready to be utilized: (1) curing of the binder following printing, (2) sintering of the green components and (3) infiltration. Each of the three thermal processes cause

dimensional variances. The objective of this study is to investigate finite element thermal-mechanical modeling in order to optimize the sinter profile and predict the final part dimension. The analytical model will eventually be used to define the sintering parameters and to determine, in the design stage, if a part geometry can be satisfactorily sintered. This paper discusses the sintering portion of the thermal aspects of the 3DP™ process.

Overview of Sintering

The microstructural evolution that occurs during sintering involves three distinct phases prior to achieving full component densification. The initial stage involves neck growth between powder particles which results in a light cohesive bond. The intermediate stage involves pore rounding, the densification of the sinter compact, and grain growth. The final stage involves the closing of pores and pore shrinkage, resulting in total densification.[2]

The complexity of sintering has yet to be completely theoretically defined, thus sintering is still referred to as a phenomenological process.[2,3] The difficulties with creating suitable sintering models involve lack of data at sintering temperature for materials, non-existent constitutive equations relative to sintering, and model verification (despite use of advanced mathematics). For example, isothermal models do not accurately model the sintering process because dilatometry experiments show that sintering occurs while ramping to the peak temperature. The level (macro- or micro-) at which the computer simulation places emphasis is also important. Concentrating the simulation of the sintering process at the micro-scale versus the macro-scale depends upon the desired quantities to be measured. Ultimately, a combination of an atomistic model (i.e., micro-level) and a finite element model (i.e., macro-level) is held by many researchers to be a useful, accurate, simulation approach.[4,5]

Initial Stage Sintering Mechanisms

Initial stage sintering produces neck growth through two different classes of sintering mechanisms: surface transport and bulk transport. Since it is possible to calculate thermal strains from measured shrinkage values, a logical starting point for the model is to focus on the bulk sintering mechanisms that produce physical shrinkage. These mechanisms include plastic flow (PF), grain boundary diffusion (GB), and volume diffusion (VD). Each mechanism is active during different stages of the sintering process so that the total shrinkage produced is the superposition of these three bulk mechanisms.[2,6]

Plastic flow can be described as nonconservative dislocation motion. It is directly related to the temperature profile and is active while the component's temperature is approaching the sintering temperature, so PF is only present during initial stage sintering and ceases once the sintering temperature is achieved.[2] The more severe ramp in temperature profile, the greater the rate in plastic flow.

Grain boundary diffusion involves the realignment of grain boundaries due to crystal misalignment. This mechanism depends primarily upon the grain size and concentration of grain boundaries per unit volume. The movement of atomic particles along the grain boundaries usually possesses an activation energy less than that of volume diffusion, and therefore is not as influential in shrinkage as volume diffusion.

Volume diffusion involves the movement of particles through lattice vacancies of a crystalline structure. The diffusion rate is dependent upon three parameters associated with the powder structure: temperature, composition, and pressure (or curvature). The evolution of neck growth from volume diffusion is essentially the redistribution of atoms within vacancy positions that leads to mass distribution between the particles. Temperature is the dominating factor controlling the concentration of vacancies; hence, the rate at which material mass may reposition is related to temperature.

The necks that form between particles during sintering produce the effective strain contribution for each of these bulk mechanisms. The neck growth and shrinkage between two equally sized spheres is represented in Figure 1 (see also Equations (1) and (2), and Table 1).

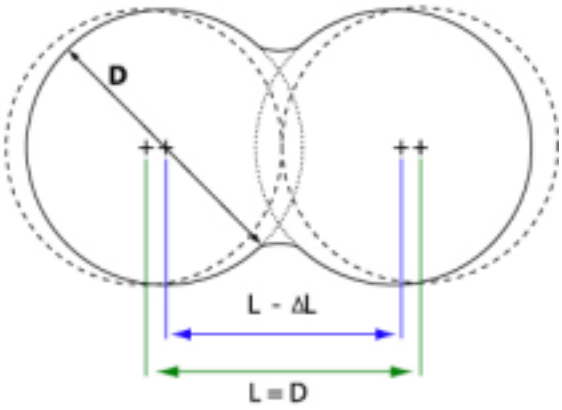

Figure 1. Schematic representation of a neck growth model for two equally sized spheres.

The effective strain (ε_i) for each mechanism follows a kinetic law as shown in Equation (1):

$$(\varepsilon_i)^{n/2} = \left(\frac{\Delta L}{L}\right)^{n/2} = \frac{Bt}{2^n D^m} \tag{1}$$

where t is time, D is particle diameter, L is the original length between the centers of the spherical particles, ΔL is the change in distance between centers, and the remaining parameters are defined in Table 1. The constant B in Equation (1) is dependant on the specific sintering mechanism being considered, and is exponentially dependent upon temperature by the relationship shown in Equation (2):

$$B = B_o \exp\left(-\frac{Q}{kT}\right) \tag{2}$$

where Q is the activation energy, and the remaining variables are defined in Table 1.

Table 1. Summary of initial-stage sintering equations and parameters for spheres.[2,5]

Mechanism	*n*	*m*	B_o
Volume Diffusion (VD)	5	3	$\frac{80\gamma D_v \Omega}{kT}$
Grain Boundary Diffusion (GB)	6	4	$\frac{20\delta\gamma D_b \Omega}{kT}$
Plastic Flow (PF)	2	1	$\frac{9\pi\gamma b D_v}{kT}$

Symbols

γ= surface energy — D_v = volume diffusivity
δ= grain boundary width — D_b = grain boundary diffusivity
Ω= atomic volume — b = Burgers vector
k = Boltzmann's constant — T = Absolute temperature

Model of a Three-Dimensionally Printed Component

The layer-by-layer construction of 3DP™ components must be considered in theoretical modeling in order to be accurate for analytical purposes. Therefore, the development of a layered simulation model is necessary to simulate the sintering process for the component. A pictorial representation of modeling a 3DP™ component for finite element analysis is shown in Figure 2.

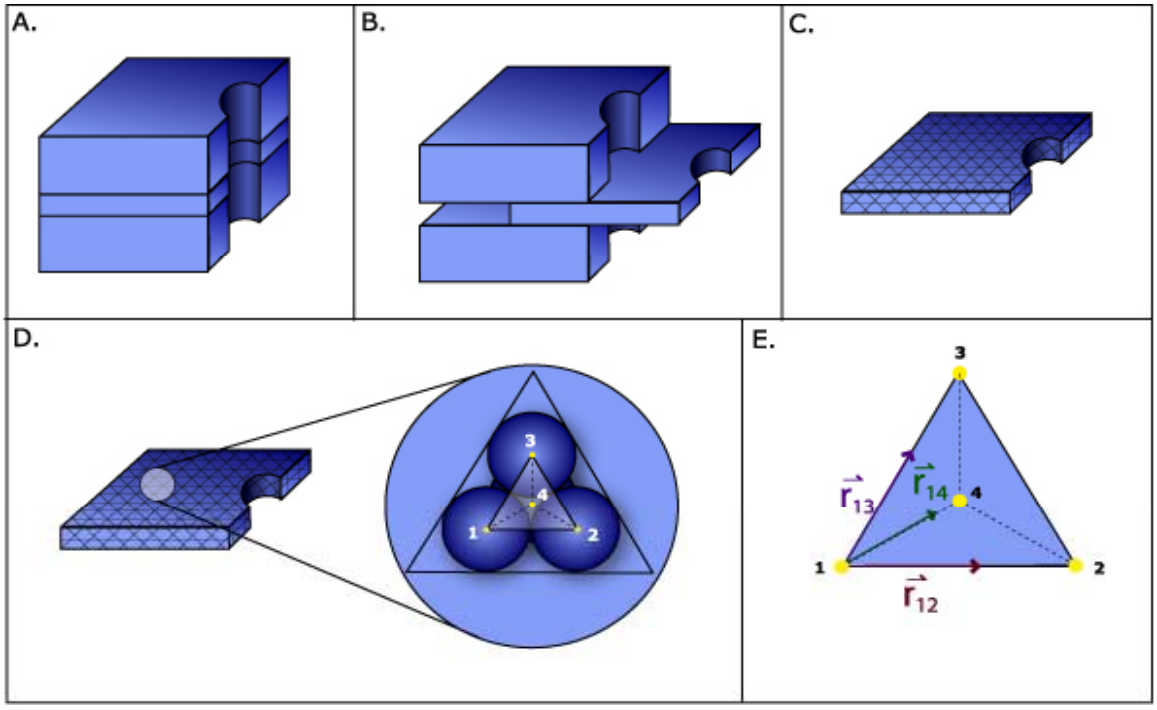

Figure 2. Pictorial representation of modeling a 3DP™ component for finite element analysis. (A) fully printed component; (B) one printed layer of the 3DP™ component; (C) tetrahedral meshing of one layer; (D) tetrahedral element comprising four powder particles; (E) elemental representation of a four-noded element.

A finite element analysis of the sintering of a 3DP™ component requires the additional analytical steps of creating and meshing a printed layer. The modeled layer corresponds to exactly one layer of the 3DP™ manufactured component. The layer is subdivided into smaller elements comprising a number of powder particles modeled as tetrahedral elements whose deformation is governed by Equation (1) and the information in Table 1. The sintering bonds produced between layers (i.e., *z*-print direction) would have less particle contact due to the compaction of the particles in this direction. This is an inherent trait of the printing process and has been observed experimentally.

EXPERIMENTAL RESULTS

Rectangular sample blocks were printed in 316L stainless steel (316L SS) and 420 stainless steel (420 SS) powder with dimensions of 25x25x40 *mm*, where the 40 *mm* dimension was oriented in each of the three (i.e., *x*-, *y*-, and *z*-) print directions. The sample blocks were measured in the green state and sintered state using a non-contact video measuring device (see Experimental Procedure).

From these measurements, the thermally induced sintering strains were determined as the normalized change in length using Equation (3). Results are shown for 316L SS and 420 SS in Figures 3 and 4, respectively.

$$\varepsilon_T = \frac{\Delta L}{L} \tag{3}$$

Statistical analysis (t-test) of the measured strains indicated that the strain produced in each of the three print directions is independent of each other for both the 316L SS and 420 SS samples. Thus, the microstructural development of the component is anisotropic.[7]

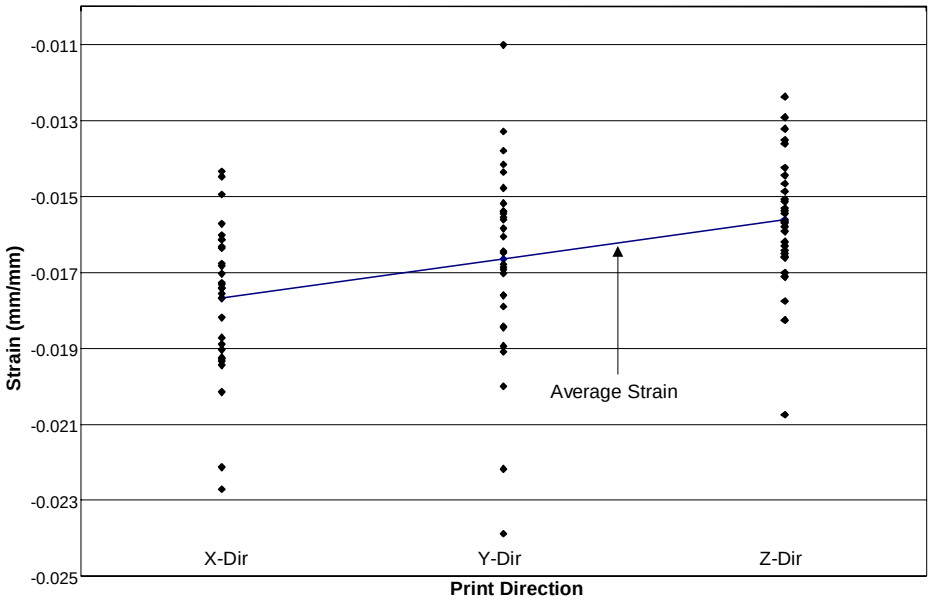

Figure 3. Sintering strains produced in 316L SS rectangular sample blocks.

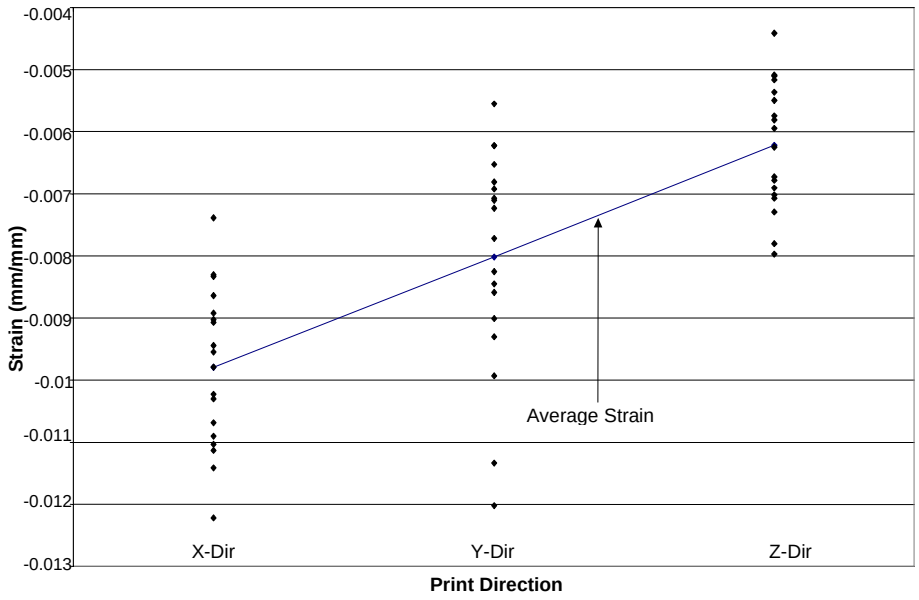

Figure 4. Sintering strains produced in 420 SS rectangular sample blocks.

The mean strain for each print direction is represented by the trendlines in Figures 3 and 4. The mean strain observed for each print direction is unique, and the differences in strain for the three print directions can be attributed to two factors inherent to the 3DP™ process: binder droplet size and print direction itself. Specifically, deviations in the *x*-direction are attributed to the start and stop of binder distribution; deviations in the *y*-direction are attributed to the jet width of the print head, which produces slight overlap for adjacent print *y* bands; and deviations in the *z*-direction are attributed to a combination of powder/binder adjacent layer adhesion and layer thickness. Further analysis of the 316L SS and 420 SS data reveals that the strain in each print direction shows small standard deviations. The normal distributions in Figures 5 and 6 indicate that although unique to print direction, the strain values are reproducible and consistent.

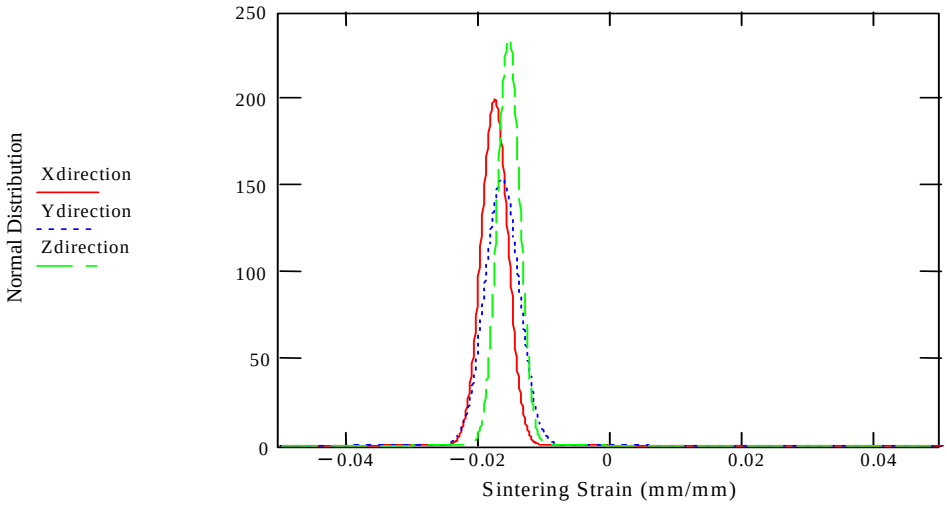

Figure 5. Normal distribution of sintering strains for 316L SS sample blocks.

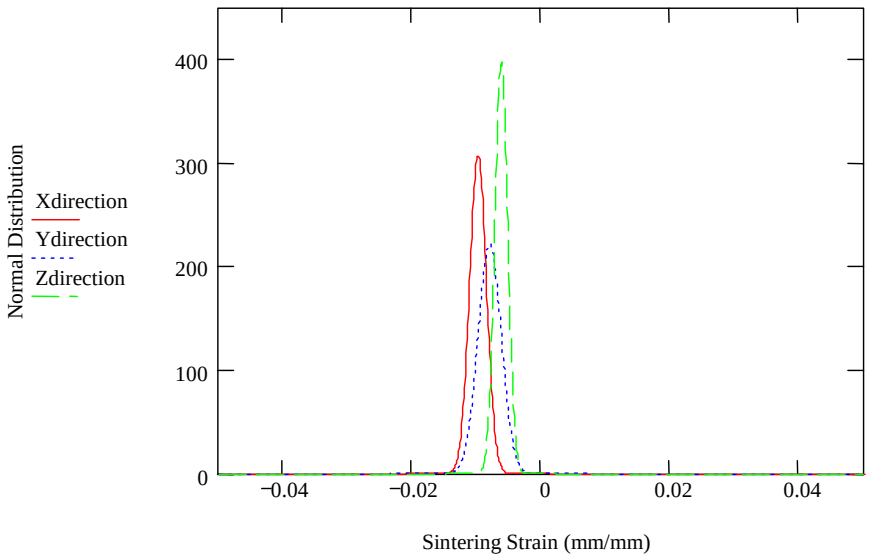

Figure 6. Normal distribution of sintering strains for 420 SS sample blocks.

CONCLUSIONS

A 3DP™ manufactured component is anisotropic; that is, it has the quality of variation of physical properties with the (*x*-, *y*-, or *z*-print) direction along which the property is measured. This anisotropic nature is related to aspects of the three-dimensional layered physical construction of the component, the effects of which are retained through thermal processing. This study introduced initial steps toward finite element thermal analysis to predict the effective strain produced from sintering 3DP™ manufactured components. The model utilizes a meshed layer procedure and incorporates both the micro-scale aspects of sintering between particles as well as the macro-scale parameters of dimensionality and strain. Due to the anisotropic construction of 3DP™ components, determination of strain in each print direction is the initial step to defining the thermally induced stresses within the component. The strains are used to predict localized stresses within the component, which in turn provides a prediction of possible positions of fracture. Consideration of the layer-by-layer construction inherit to the 3DP™ manufacturing technique is essential in order to correctly simulate as many process traits as possible, providing for a useful, accurate modeling tool for the 3DP™ process.

EXPERIMENTAL PROCEDURE

Components were manufactured on a ProMetal RTS-300, a solid freeform fabrication machine capable of creating metal components as large as 12x12x10 *in*. Typical process speed is 10-20 in^3/hr, depending on resolution. Components were thermally processed in a nonvacuum atmosphere furnace. Metal powders and binder were used as obtained from commercial vendor (Extrude Hone Corporation, Irwin, PA).

Dimensional measurements were obtained using a Smart Scope non-contact video measuring device (Optical Gaging Products, Inc.). The Smart Scope measuring method selects several

points along each edge of the sample at a magnification of 53x. A least squares linear fit is used for the edges of the samples. Dimensional measurements are calculated from the linear fit lines with an accuracy of $\pm 40 \mu m$ (0.00015 *in*).

ACKNOWLEDGEMENTS

Financial support for this work is provided by the Office of Naval Research, Contract #N00014-C-00-0378. The authors are grateful to Bill Pedersen (University of Washington) for assistance with experimental data interpretation, and the Physics Department at University of Washington for equipment use. We also thank Angela Wilson for graphic design assistance, Dawn Buckley and Melinda Webel for editorial assistance.

REFERENCES

1. 3DP is a registered trademark of the Massachusetts Institute of Technology.

2. R. M. German, *Sintering Theory and Practice*, Wiley & Sons, New York, 1996.

3. E. A. Olvesky, *Theory of Sintering: from discrete to continuum*, Material Science and Engineering: R, Reports, Vol. R23, Issue 2, June 1998, pp.41-100.

4. R. M. German, personal communication and presentation, Critical Overview of Sintering Computer Simulations, at The 2002 World Congress on Powder Metallurgy & Particulate Materials, Orlando, FL, June 2002.

5. E. A. Olvesky, personal communication and presentation, Sintering of Functionally Gradient Ceramic Freeforms, and presentation, Sintering of Multilayer Powder Composites: Distortion and Damage Control" at the 2002 World Congress on Powder Metallurgy & Particulate Materials, Orlando, FL, June 2002.

6. Powder Metal Technologies and Applications, ASM Handbook, Volume 7, 1998 pp.448-452.

7. A. P. Boresi, R. J. Schmidt, and O. M. Sidebottom, *Advanced Mechanics of Materials*, 5th Edition, Wiley & Sons, 1993.